Journal of Biomolecular NMR, 6 (1995) 237–244
ESCOM

J-Bio NMR 299

Determination of $^3J(H_i^N,C_i')$ coupling constants in proteins with the C'-FIDS method

A. Rexroth[a], S. Szalma[b], R. Weisemann[c], W. Bermel[c], H. Schwalbe[d] and C. Griesinger[a,*]

[a]*Institut für Organische Chemie, Universität Frankfurt, Marie Curie Strasse 11, D-60439 Frankfurt, Germany*
[b]*Biosym Technologies Inc., 9685 Scranton Road, San Diego, CA 92121-3752, U.S.A.*
[c]*Bruker Analytische Messtechnik GmbH, Silberstreifen, D-76287 Rheinstetten, Germany*
[d]*University of Oxford, New Chemistry Laboratory, South Parks Road, Oxford OX1 3QT, U.K.*

Received 11 May 1995
Accepted 27 July 1995

Keywords: Multidimensional NMR; Protein structure; ^3J coupling constants; C'-FIDS method; 2D C'-FIDS-HSQC; 3D C'-FIDS-HNCO; 3D C'-FIDS-HNCO-E.COSY; Isotope labeling; Rhodniin

Summary

We introduce the C'-FIDS-$^1H,^{15}N$-HSQC experiment, a new method for the determination of $^3J(H_i^N,C_i')$ coupling constants in proteins, yielding information about the torsional angle ϕ. It relies on the $^1H,^{15}N$-HSQC or HNCO experiment, two of the the most sensitive heteronuclear correlation experiments for isotopically labeled proteins. A set of three $^1H,^{15}N$-HSQC or HNCO spectra are recorded: a reference experiment in which the carbonyl spins are decoupled during t_1 and t_2, a second experiment in which they are decoupled exclusively during t_1 and a third one in which they are coupled in t_1 as well as t_2. The last experiment yields an E.COSY-type pattern from which the $^2J(H_i^N,C_{i-1}')$ and $^1J(N_i,C_{i-1}')$ coupling constants can be extracted. By comparison of the coupled multiplet (obtained from the second experiment) with the decoupled multiplet (obtained from the first experiment) convoluted with the $^2J(H_i^N,C_{i-1}')$ coupling, the $^3J(H_i^N,C_i')$ coupling can be found in a one-parameter fitting procedure. The method is demonstrated for the protein rhodniin, containing 103 amino acids. Systematic errors due to differential relaxation are small for $^nJ(H^N,C')$ couplings in biomacromolecules of the size currently under NMR spectroscopic investigation.

Introduction

In protein structure elucidation, the determination of coupling constants has become increasingly important. Coupling constants provide information about local conformations and complement the structural information obtained from NOEs (Neri et al., 1989; Garret et al., 1994; Karimi-Nejad et al., 1994). A number of different principles for the determination of coupling constants have been introduced over the last years, among which are E.COSY-derived methods (Griesinger et al., 1985, 1986,1987), methods relying on fitting procedures (Keeler et al., 1988,1989; Keeler and Titman, 1990) and techniques based on the 'intensity method' (Bax et al., 1992; Blake et al., 1992; Grzesiek et al., 1993; Vuister and Bax, 1993a,b; Vuister et al., 1993a,b; Zhu and Bax, 1993). Here we introduce a novel, very sensitive method to measure $^3J(H_i^N,C_i')$ coupling constants in proteins employing a FIDS (fitting of doublets and singlets) procedure (Schwalbe et al., 1993,1994). $^3J(H_i^N,C_i')$ coupling constants can be used in protein structure calculations from NMR data as experimental ϕ-angle constraints, which will lead to better defined structures. $^2J(H_i^N,C_{i-1}')$ and $^1J(N_i,C_{i-1}')$ coupling constants, which can also be extracted from the set of spectra introduced in this paper, contain information both about the neighbouring backbone torsional angles as well as bond lengths and thus hydrogen bonds (Delaglio et al., 1991; Edison et al., 1994a,b; Juranic et al., 1995).

Methods

The FIDS method for determining an $^nJ(I,S)$ coupling is based on the idea of recording two different spectra of

*To whom correspondence should be addressed.

a

b

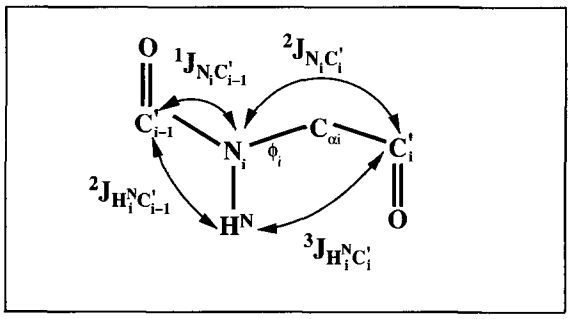

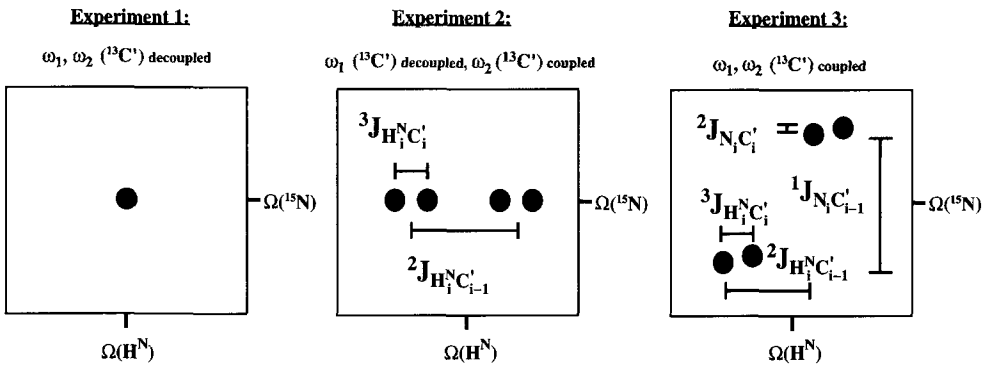

Fig. 1. (a) Pulse sequences for the determination of $J(H^N,C')$ coupling constants from C'-FIDS-^{1}H,^{15}N-HSQC experiments. In Experiment 1, the aliphatic carbon and the carbonyl resonances were decoupled during t_1 and t_2 and the nitrogen resonances during t_2. Experiment 2 was performed in the same way as Experiment 1, except that the C' coupling was retained during t_2. In Experiment 3 the carbonyl resonances were decoupled neither in t_1 nor in t_2. The carbon carrier frequency was placed in the middle of the C^α range (82.29 ppm). The ^{15}N spins were decoupled using the GARP (Shaka et al., 1985) sequence. In order to obtain the same line shape in Experiments 1 and 2, carbon decoupling was accomplished with an MLEV-16 expansion of a superposition of an on-resonance G3 pulse (Emsley and Bodenhausen, 1989,1990) and a G3 pulse that was cosine modulated with 20 kHz (Experiment 1) and 50 kHz (Experiment 2), respectively (Eggenberger et al., 1992a). For all C' and aliphatic carbon-selective 180° pulses, G3 Gaussian pulse cascades (Emsley and Bodenhausen, 1989,1990) of 256 μs pulse duration were used. Pulses on C' were performed by phase modulation. The delays were: $\Delta = 5.4$ ms, $\Delta' = 1.703$ ms, $\tau_g = 3.724$ ms. The phase cycling employed was as follows: $\phi_1 = x,-x$; $\phi_2 = x,x,-x,-x$; $\phi_3 = x,-x,-x,x,-x,x,x,-x$. Eight scans per t_1 increment (1000 experiments, $t_1^{max} = 540$ ms, spectral width 1852 Hz) were recorded with 1024 complex points in t_2 (spectral width 4000 Hz) for Experiments 1 and 2. In Experiment 3, 400 experiments with $t_1^{max} = 216$ ms were recorded. The coherence transfer from nitrogen to protons was accomplished with a COS-INEPT (Palmer et al., 1991; Muhandiram et al., 1993; Schleucher et al., 1993; Muhandiram and Kay, 1994) in conjunction with a heteronuclear gradient echo. The durations and strengths of the gradients were as follows: $G_1 = (3.2$ ms, 49.5 G/cm), $G_2 = (1.6$ ms, ±10.1 G/cm), $\psi = \pm y$ for echo and antiecho selection. The sign of the gradient G_2 and the phase ψ were reversed simultaneously every second scan, and the resulting FIDs were stored separately. The recovery delay was 200 μs for both gradients. (b) Schematic representation of the spectra obtained from the three experiments described in (a): Experiment 1 yields a singlet with respect to the couplings to C', Experiment 2 a doublet of doublets. Experiment 3 yields a four-spin E.COSY-type pattern with little displacement in ω_1, owing to the almost vanishing $^2J(N_i,C'_i)$ coupling, but large displacement due to the $^1J(N_i,C'_{i-1})$ coupling of about −15 Hz, which renders exact values for the $^2J(H_i^N,C'_{i-1})$ couplings.

an I spin. In one spectrum, the S spin is selectively decoupled and the spectrum of the I spin shows a singlet with respect to the $^nJ(I,S)$ coupling. In the second experiment, the S spin is not decoupled and the spectrum of the I spin shows a doublet with respect to the $^nJ(I,S)$ coupling. The desired $^nJ(I,S)$ coupling can be obtained by convoluting the decoupled I spin spectrum with a trial coupling J^{trial} and determining the difference between the convoluted spectrum and the coupled spectrum. This constitutes a one-dimensional fitting procedure that is robust against systematic errors, even if the coupling constant is small compared to the line width (Schwalbe et al., 1993). If the abundance of the S spin is smaller than 100%, then the spectrum recorded without decoupling of the S spin will also contain the I spin singlet with respect to the $^nJ(I,S)$ coupling. Corrections, however, can be made in the procedure for the extraction of the coupling constant, provided the abundance of the S spin is known. The relative error introduced on the coupling and the relative error in the determination of the abundance of the $^{13}C'$ spins causing the former error are approximately identical.

For the application of the FIDS method to the determination of $^3J(H_i^N,C_i')$ coupling constants in uniformly labelled proteins, one has to consider that the coupled H_i^N-spectrum is a doublet of doublets (Experiment 2 in Fig. 1b) due to the evolution of both the $^2J(H_i^N,C_{i-1}')$ and the $^3J(H_i^N,C_i')$ coupling, which are of the same order of magnitude (~5 Hz) (Fig. 1b). Since it is impossible to fit two coupling constants that are smaller than the line width, a third experiment is needed that allows the measurement of either the $^2J(H_i^N,C_{i-1}')$ or the $^3J(H_i^N,C_i')$ coupling individually. The determination of the $^2J(H_i^N,C_{i-1}')$ coupling is possible in an $^1H,^{15}N$-E.COSY-type correlation experiment, since this coupling is associated with the $^1J(N_i,C_{i-1}')$ coupling of ~15 Hz, whereas the $^3J(H_i^N,C_i')$ coupling is associated with the rather small $^2J(N_i,C_i')$ coupling constant (Fig. 1b).

TABLE 1
EXPERIMENTS FOR THE DETERMINATION OF HETERONUCLEAR COUPLING CONSTANTS TO C'

$^1H^N,^{15}N$-HSQC	C' in ω_1	C' in ω_2
Experiment 1	decoupled	decoupled
Experiment 2	decoupled	coupled
Experiment 3	coupled	coupled

Hence we propose to record a $^1H,^{15}N$-HSQC experiment (Fig. 1a) in which the carbonyl spins are decoupled during t_1 as well as during t_2 (Experiment 1) and a second experiment in which they are decoupled exclusively in t_1 (Experiment 2). The first experiment yields a singlet with respect to the $J(H^N,C')$ couplings for the H_i^N-spectrum (Fig. 1b, left) and the second results in a doublet of doublets, due to the $^2J(H_i^N,C_{i-1}')$ and $^3J(H_i^N,C_i')$ couplings (Fig. 1b, middle). As previously described (Delaglio et al., 1991; Madsen et al., 1993), the $^2J(H_i^N,C_{i-1}')$ coupling, which is associated with the $^1J(N_i,C_{i-1}')$ coupling, can be determined from the E.COSY-type pattern (Fig. 1b, right) obtained in a $^1H,^{15}N$-HSQC without decoupling of the C' in t_1 and t_2 (Experiment 3).

The method can be extended to a third dimension in case of overlap, as will be demonstrated in a set of 3D C'-FIDS-HNCO experiments.

Measurement of $^3J(H_i^N,C_i')$, $^2J(H_i^N,C_{i-1}')$ and $^1J(N_i,C_{i-1}')$ coupling constants in 2D C'-FIDS-$^1H,^{15}N$-HSQC experiments

To determine the $^3J(H_i^N,C_i')$, $^2J(H_i^N,C_{i-1}')$ and $^1J(N_i,C_{i-1}')$ coupling constants, three experiments were recorded (see Table 1). The corresponding pulse sequences are shown

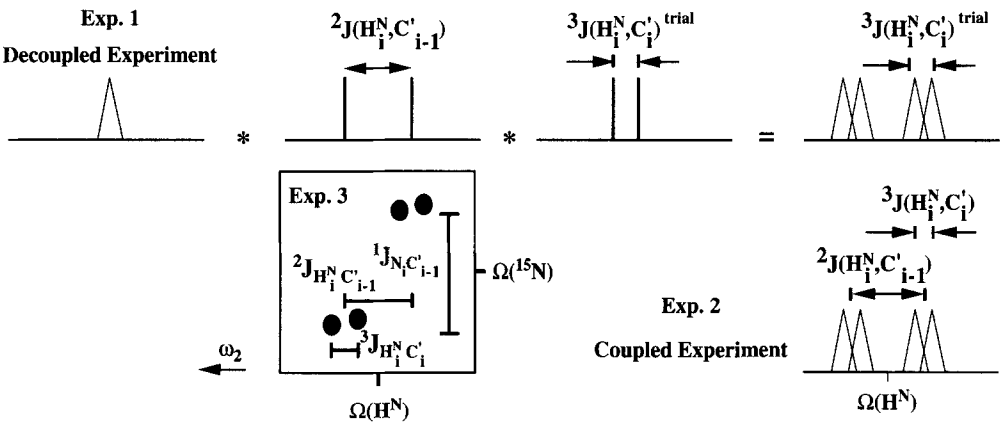

Fig. 2. Application of the FIDS method to the determination of $^3J(H_i^N,C_i')$ coupling constants. The H_i^N proton couples to the C' spin of its own amino acid residue via a $^3J(H_i^N,C_i')$ coupling as well as to the C' spin of the preceding amino acid via the $^2J(H_i^N,C_{i-1}')$ coupling. Therefore, the C'-coupled H_i^N spectrum (Experiment 2) shows a doublet of doublets due to these two $J(H^N,C')$ coupling constants. The C'-decoupled H_i^N spectrum shows a singlet. Since the $^2J(H_i^N,C_{i-1}')$ coupling constant is known, the C'-decoupled H_i^N spectrum can be convoluted, first with an in-phase stick doublet of the $^2J(H_i^N,C_{i-1}')$ coupling and then with the trial coupling constant J^{trial} for $^3J(H_i^N,C_i')$. When J^{trial} equals the desired coupling constant, the difference is minimal.

in Fig. 1a. The decoupling of the carbonyls and the aliphatic carbons was accomplished by an MLEV-16 expansion of a superposition of an on-resonance G3 pulse and a G3 pulse that is cosine modulated with 20 kHz (Experiment 1) and 50 kHz (Experiment 2), respectively (Eggenberger et al., 1992a). Figure 1b shows the schematic multiplet structures expected. From the E.COSY-type spectrum (Experiment 3), the $^2J(H_i^N,C'_{i-1})$ coupling can be extracted either by inspection or by fitting. The $^3J(H_i^N,C'_i)$ coupling is determined in the following way (Fig. 2): the ω_2 trace derived from the fully decoupled spectrum (Experiment 1) is convoluted with a stick doublet of the $^2J(H_i^N,C'_{i-1})$ coupling obtained from the E.COSY spectrum. The doublet obtained is further convoluted with a trial coupling $^3J(H_i^N,C'_i)^{trial}$ and yields a doublet of doublets (Fig. 2). The integral of the power spectrum of the difference between the doubly convoluted trace and the coupled trace obtained from Experiment 2 is at a minimum if the trial coupling matches the observed coupling $^3J(H_i^N,C'_i)^{trial} = {}^3J(H_i^N,C'_i)$. The stick doublets have an integral 1/2 for each component.

The fitting of the desired coupling constants was done in the time domain using FELIX macros. First, the two submultiplets in the E.COSY-type spectrum (Experiment 3) were summed along identical distances in the ^{15}N-dimension. We chose integration limits about twice as large as the line width in ω_1, in order to obtain optimal signal-to-noise ratios in the ω_2 traces. In cases of overlap, single traces have been used as well. The imaginary part of the two resulting 1D submultiplets was recovered by a Hilbert transformation and the two submultiplets in the time domain were generated by inverse FT. Linear phase correction in the time domain, equivalent to frequency shifting in the frequency domain, was used to minimize the rms difference of the two submultiplets. The optimal linear phase correction found was translated into the $^2J(H_i^N,C'_{i-1})$ coupling. In the second step, the $^3J(H_i^N,C'_i)$ coupling was determined in the following way: the corresponding cross peaks in the fully decoupled spectrum (Experiment 1 in Fig. 1b) and in the spectrum without ω_2 decoupling (Experiment 2) were summed up along identical ω_1 frequency windows, yielding a ω_2 trace. The complex time-domain data of the trace obtained from the fully decoupled spectrum were generated by Hilbert and inverse Fourier transformation. These time-domain data were multiplied with a cosine modulation according to the previously determined $^2J(H_i^N,C'_{i-1})$ coupling. The time-domain data were further multiplied with the cosine modulation of the trial coupling $^3J(H_i^N,C'_i)^{trial}$ and yielded time-domain data containing two cosine modulations. Again, the rms of the difference between the latter time-domain data and the time-domain data obtained for Experiment 2 was minimized, yielding the optimum value for $^3J(H_i^N,C'_i)^{trial}$ that was taken as the experimental $^3J(H_i^N,C'_i)$ coupling constant.

Extension of the C'-FIDS method to a third dimension: 3D C'-FIDS-HNCO and 3D C'-FIDS-HNCO-E.COSY

The C'-FIDS method can be incorporated into a 3D HNCO experiment in a straightforward manner. The pulse sequences used are shown in Fig. 3. As in the two-dimensional version, the C'-decoupled and C'-coupled experiments were recorded in an interleaved manner. The pulse sequence used (Fig. 3a) is a modified version of the standard HNCO experiment introduced by Kay and Bax (Kay et al., 1990; Bax and Ikura, 1991).

The generation of the E.COSY pattern with C' as passive spin, necessary in the third experiment, requires some modifications in the ^{15}N evolution period: the anti-phase coherence of the ^{15}N spins at the beginning of the ^{15}N evolution time should evolve under the $^1J(N_i,C'_{i-1})$ coupling during $1/(2\,{}^1J(N_i,C'_{i-1})) + t_2$ in order to generate an in-phase E.COSY pattern with respect to C'. However, since the evolution time t_2^{max} must be larger than $2\tau''$ to resolve the $^1J(N_i,C'_{i-1})$ coupling constant, we used a semi-constant time evolution period (Grzesiek and Bax, 1993), as shown in Fig. 3b. The following delays were chosen: $t_2^a = a\,t_2$, with $a = \tau''/t_2^{max}$, and $\tau'' = 1/(4\,{}^1J(N,C'))$.

The maximum evolution time t_2^{max} was chosen to be $2/{}^1J(NC') = 133$ ms. The ^{15}N chemical shift evolution takes place during $-t_2$. The heteronuclear $^1J(N_i,C'_{i-1})$ coupling evolves during the period $2\tau'' - t_2$, whereas evolution of the $J(N,C^\alpha)$ couplings is prevented.

The coupling constant extraction for the 3D version was made using the same FELIX macro-based approach as for the evaluation of the 2D spectra. To obtain the traces along ω_3, summations were carried out along the ω_1 (^{15}N) and ω_2 (^{13}C) dimensions before transforming to the time domain.

Results and Discussion

The C'-FIDS method has been applied to the protein rhodniin, containing 103 amino acids. In Fig. 4a, the E.COSY-type peaks obtained from the 2D C'-FIDS-^1H, ^{15}N-HSQC (Experiment 3 in Figs. 1 and 2) for Val^{93}, Asp^{77}, Asp^{61} and Cys^{27} are shown, giving the values of the $^1J(N_i,C'_{i-1})$, $^2J(H_i^N,C'_{i-1})$ and $^3J(H_i^N,C'_i)$ coupling constants as indicated.

The fitting of the $^3J(H_i^N,C'_i)$ couplings can be done in a reliable way, as is demonstrated in Fig. 4b, where the different traces used during the fitting procedure outlined above are shown. Plotted are the coupled spectrum (A) obtained from Experiment 1, the decoupled spectrum (B) obtained from Experiment 2 and the three difference spectra, i.e., before convolution (C), after the convolution with $^2J(H_i^N,C'_{i-1})$ obtained from Experiment 3 (D), and after further convolution with the optimal trial coupling (E), together with the corresponding power integrals (taking the limits as indicated by vertical lines). The integral value of the reference trace was calibrated to a value

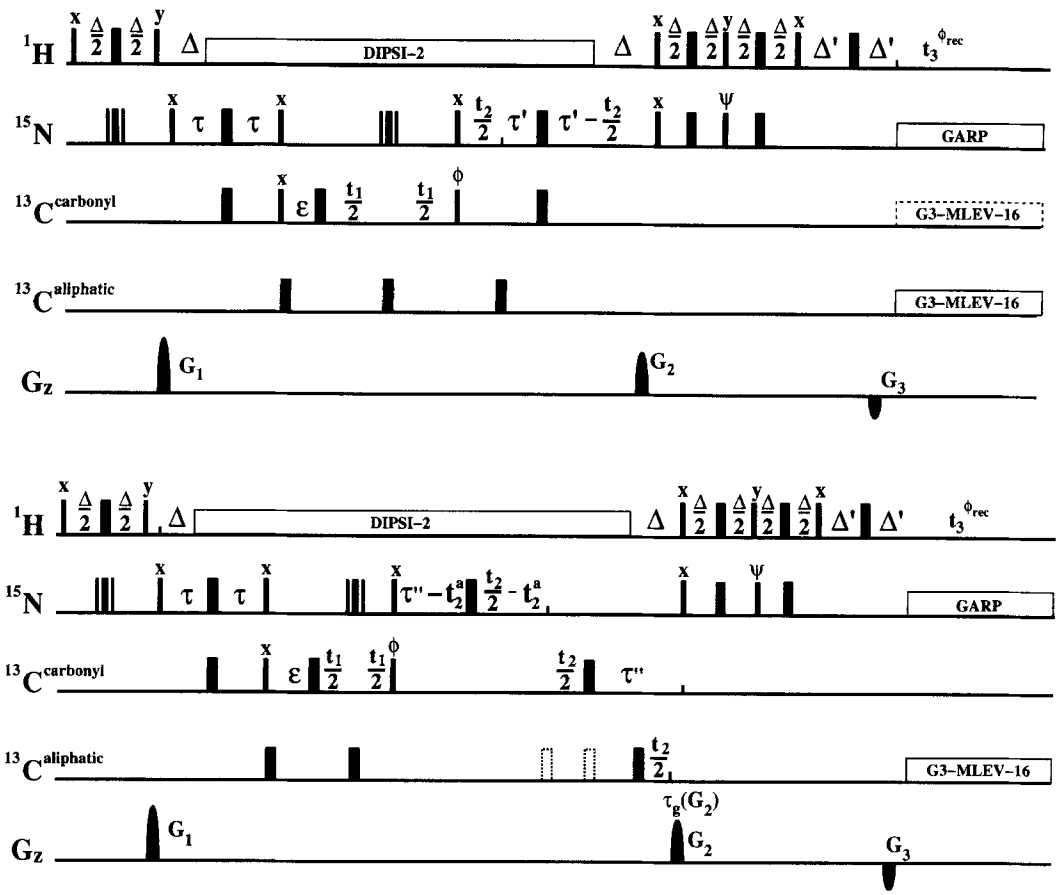

Fig. 3. (a) Pulse sequence for the determination of $^3J(H_i^N,C_i')$ coupling constants in a 3D C'-FIDS-HNCO experiment. The delays are as follows: $\Delta = 5.2$ ms, $\tau = 13.7$ ms, $\tau' = 14.7$ ms, $\Delta' = 2.203$ ms, $\varepsilon = 77$ μs (compensation for composite 180° (^{15}N)). Phase cycling was as follows: $\phi = x,-x$; $\phi_{rec} = x,-x$. Two scans were recorded per t_1 (128 experiments, $t_1^{max} = 84.486$ ms, spectral width 1515 Hz), t_2 experiment (140 experiments, $t_2^{max} = 19.396$ ms, spectral width 1805 Hz) with 1024 complex points in t_3 (spectral width 4000 Hz). As in the 2D version, the coherence transfer from nitrogen to protons was accomplished with a COS-INEPT. The durations and strengths of the gradients were as follows: $G_1 = (4$ ms, 38.5 G/cm, 1 ms recovery), $G_2 = (4$ ms, 49.5 G/cm, 500 μs recovery), $G_3 = (2$ ms, ±10.1 G/cm, 200 μs recovery), $\psi = \pm y$ for echo and antiecho selection. The sign of the gradient G_3 and the phase ψ were reversed simultaneously every second scan, and the resulting FIDs were stored separately. The C' resonances were decoupled and not decoupled, respectively (indicated by broken lines for decoupling), as in the 2D experiment. G4 and time-reversed G4 pulses were used in an alternating manner (Eggenberger et al., 1992b). The final matrices contained 128×256×4096 real points. In the ω_3 (proton) dimension, the final digitization achieved was 0.5 Hz. The total measuring time was 9.2 h for each experiment. The reference experiment and the coupled experiment were recorded in an interleaved way. Bloch–Siegert shifts of C' were compensated for by the two C^α selective inversion pulses during t_1. (b) Pulse sequence for the determination of $^1J(N_i,C_{i-1}')$ and $^2J(H_i^N,C_{i-1}')$ coupling constants in a 3D-C'-FIDS-HNCO-E.COSY experiment. The same parameters as in (a) were used, except for: $t_2^a = a\,t_2$, $a = \tau''/t_2^{max}$, $\tau'' = 16.67$ ms. To allow for simultaneous refocussing of the ^{15}N,^{13}C' antiphase coherence and carbonyl decoupling, ^{15}N evolution was accomplished in a semi-constant time manner. The increments were set as follows: $\Delta t_2^a = 67.67$ μs, $\Delta t_2 = 270$ μs. Bloch–Siegert shifts on C' in t_1 were compensated for by two 180° pulses, selective on $C^{aliphatic}$. In the semi-constant time evolution period t_2, two $C^{aliphatic}$ selective pulses (shown with broken lines) were used to refocus the $^1J(N,C^\alpha)$ coupling completely. Alternatively, a single 180° ($C^{aliphatic}$) pulse should be more convenient when placed $t_2/2 + \tau(G_2)$ before the N→H transfer, resulting in an evolution of the $^1J(N,C^\alpha)$ coupling during $\tau(G_2)$ for all t_1,t_2 values. Phase cycling was similar as in (a). Two scans were recorded per t_1 (32 experiments, $t_1^{max} = 21.126$ ms, spectral width 1515 Hz), t_2 experiment (246 experiments, $t_2^{max} = 133$ ms, spectral width 1852 Hz), with 1024 complex points in t_3 (spectral width 4000 Hz).

of 1. In all cases the integral decreased after every convolution step.

In the proton dimension the digital resolution was 0.5 Hz. The statistical error of the $^2J(H_i^N,C_{i-1}')$ and $^3J(H_i^N,C_i')$ coupling constants was determined in the following way: noise traces from nine different signal-free regions of the spectrum were added to the traces used to derive the coupling constants. Thus, 10 values were obtained from these traces for the two coupling constants, from which the mean value and the standard deviation of the coupling constants were calculated. The $^1J(N_i,C_{i-1}')$ coupling can be determined to an accuracy of ±0.9 Hz. As shown previously (Schwalbe et al., 1993), the fitting procedure is robust, even if the line width of the proton resonances is larger than the coupling to be determined. Table 2 shows sets of values for the three different couplings obtained from the 2D and 3D experiments. Some representative cross peaks obtained from the 3D C'-FIDS-HNCO-E.COSY experiment are shown in Fig. 4c. The coupling constants derived from the 2D and 3D versions are repro-

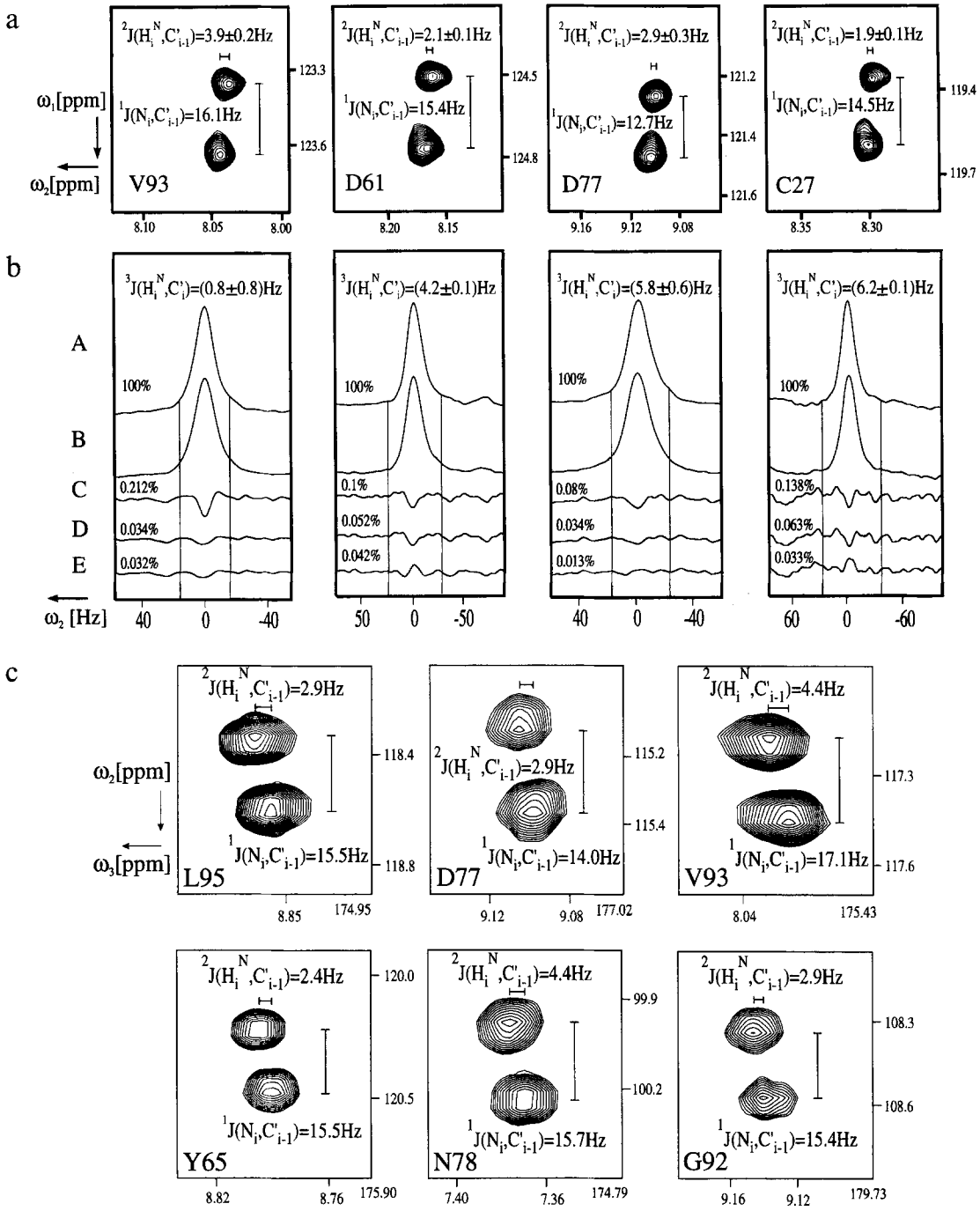

Fig. 4. (a) $^1H,^{15}N$ cross peaks of four representative amino acid residues, showing the characteristic E.COSY-type pattern. Couplings $^1J(N,C'_{i-1})$ and $^2J(H_i^N,C'_{i-1})$ were determined as indicated. The spectra were recorded on a Bruker AMX-600 spectrometer equipped with a gradient triple resonance broadband probe (TBI) at 300 K. The rhodniin sample had a concentration of 1.5 mM. The E.COSY-type spectrum was acquired within 4 h. The reference and the coupled spectrum were recorded overnight in an interleaved manner. Data processing was accomplished with FELIX using a cosine-squared apodisation in both dimensions. The final matrices contained 2048×8192 real points, resulting in digital resolutions of 0.5 Hz in the proton dimension (spectral width 4000 Hz) and 0.9 Hz in the nitrogen dimension (spectral width 1852 Hz). (b) ω_2 traces through the $^1H_i^N,^{15}N_i$ cross peaks of the C'-FIDS-$^1H,^{15}N$-HSQC spectra from Experiments 1 and 2, as described in the text. To show the effect of the fitting procedure, the difference spectra C, D and E were expanded in the vertical dimension by a factor of 4. A: reference spectrum (Experiment 1); B: fully coupled spectrum (Experiment 2); C: difference spectrum B – A; D: difference spectrum B – {A * $^2J(H_i^N,C'_{i-1})$}, where $^2J(H_i^N,C'_{i-1})$ is the coupling constant determined in the first step of the fitting procedure from the E.COSY spectrum (Experiment 3); E: difference spectrum B – {A * $^2J(H_i^N,C'_{i-1})$ * $^3J(H_i^N,C'_i)$}, where $^3J(H_i^N,C'_i)$ is the optimized value for $^3J(H^N,C')^{trial}$ as obtained in the second step of the fitting procedure (* symbolizes convolution in this context). (c) Cross peaks obtained from the 3D experiment shown in Fig. 3b. The couplings of interest are determined in the $^1H,^{15}N$ dimension, as indicated. Data were processed with FELIX using a cosine-squared apodisation in both dimensions. The final matrix for the determination of the $^2J(H_i^N,C'_{i-1})$ coupling constant contained 128×256×4096 real points. The final digitization in the ω_3 (proton) dimension was 0.5 Hz. For the determination of the $^1J(N_i,C'_{i-1})$ coupling, data were processed to a final matrix size of 64×2048×1024 real points, giving a digital resolution of 0.9 Hz in ω_1. The total measuring time was 17 h.

TABLE 2
HETERONUCLEAR COUPLING CONSTANTS TO C' FOR RHODNIIN DETERMINED WITH THE C'-FIDS TECHNIQUE

Residue	$^1J(N_i,C'_{i-1})$ (Hz)		$^2J(H_i^N,C'_{i-1})$ (Hz)		$^3J(H_i^N,C'_i)$ (Hz)		Residue	$^1J(N_i,C'_{i-1})$ (Hz)		$^2J(H_i^N,C'_{i-1})$ (Hz)		$^3J(H_i^N,C'_i)$ (Hz)	
	2D	3D	2D	3D	2D	3D		2D	3D	2D	3D	2D	3D
Gly[3]	16.3	16.4	4.4	4.9	0	1.4	Asp[55]	–	15.2	–	1.0	–	7.8
Glu[4]	15.9	15.8	4.9	3.9	–	3.4	Val[56]	–	15.5	–	1.0	–	2.2
Cys[6]	12.9	13.6	1.5	1.0	2.8	2.0	Cys[57]	14.4	14.7	4.2	5.8	3.4	2.9
Cys[8]	16.3	16.1	2.0	1.5	6.4	5.2	Gln[58]	15.6	15.5	2.9	2.4	6.0	5.0
His[10]	13.6	15.0	2.5	2.4	4.8	4.8	Asp[61]	15.0	15.0	2.1	2.4	4.2	4.8
Ala[11]	16.5	–	4.9	–	3.6	–	Gly[62]	15.1	16.1	4.2	2.9	3.8	3.4
Leu[12]	14.8	15.6	3.4	3.9	6.8	7.8	Asp[63]	15.8	15.5	4.3	4.4	2.0	2.4
Val[15]	14.6	15.5	2.9	1.9	6.6	7.6	Tyr[65]	15.0	15.5	2.5	2.4	5.2	5.4
Cys[16]	15.5	–	0.1	–	7.2	–	Lys[66]	15.3	15.1	5.3	5.4	0	1.0
Gly[17]	15.8	15.7	4.9	3.9	1.4	1.6	Val[68]	16.0	15.9	3.4	3.9	3.2	2.4
Ser[18]	12.9	14.0	4.8	4.4	0.8	1.0	Cys[69]	15.7	14.9	5.3	5.4	0.6	0.8
Asp[19]	16.1	15.5	3.5	3.9	7.0	7.8	Gly[70]	15.4	15.2	4.3	4.9	2.0	3.6
Gly[20]	16.9	15.8	6.0	5.9	0	1.8	Ser[71]	13.2	14.2	4.6	4.4	1.0	0.6
Glu[21]	–	16.0	–	6.6	–	3.4	Asp[73]	16.3	15.5	4.9	4.9	3.6	3.8
Thr[22]	15.0	15.4	0.6	1.6	5.3	5.9	Ile[74]	15.1	–	2.6	–	5.0	–
Tyr[23]	13.4	–	2.0	–	4.0	–	Thr[75]	13.8	14.6	3.9	3.9	1.6	0.8
Ser[24]	12.8	14.8	2.9	3.9	5.6	6.2	Tyr[76]	15.3	16.3	2.4	2.4	5.2	–
Asn[25]	16.8	16.4	4.0	3.4	8.0	9.0	Asp[77]	12.6	14.0	2.9	2.9	4.4	5.8
Cys[27]	14.7	–	6.2	–	1.9	–	Asn[78]	16.5	15.7	4.4	4.4	6.4	6.4
Thr[28]	14.7	15.7	3.9	4.4	1.4	2.6	Asn[79]	15.3	15.5	4.4	3.9	–	3.6
Leu[29]	15.0	15.2	3.4	3.9	4.6	3.6	Arg[81]	15.5	15.1	2.9	2.4	2.2	1.2
Asn[30]	14.1	15.0	1.0	0.5	6.0	5.4	Leu[82]	15.1	15.5	1.9	2.0	4.2	4.4
Cys[31]	14.5	15.0	3.6	2.9	7.2	6.0	Glu[83]	–	16.5	–	4.4	–	8.8
Ala[32]	14.4	15.4	4.6	4.9	0.8	1.8	Cys[84]	14.9	15.8	1.4	1.5	4.8	3.0
Lys[33]	14.8	15.2	1.8	1.5	7.2	7.0	Ala[85]	–	13.2	–	1.4	–	4.8
Phe[34]	15.0	15.3	3.9	3.4	0	0.8	Ser[86]	16.3	15.4	1.5	0.5	1.0	–
Asn[35]	15.4	15.8	4.0	4.0	–	7.8	Ile[87]	15.2	15.0	3.0	2.4	1.6	2.6
Gly[36]	15.4	15.9	4.8	4.4	0.8	0.8	Ser[88]	–	17.0	–	2.9	–	4.6
Lys[37]	16.3	15.5	2.1	3.4	4.2	5.2	Ser[90]	16.2	–	4.4	–	4.4	–
Glu[39]	15.1	15.2	3.9	3.9	7.6	6.0	Gly[92]	15.6	15.4	2.4	2.9	2.6	3.6
Leu[40]	15.8	15.3	5.8	4.8	3.0	4.4	Val[93]	16.1	17.1	3.9	4.4	0.8	0.6
Val[41]	14.4	–	4.3	–	0.6	–	Glu[94]	–	16.2	–	5.3	–	1.0
Lys[42]	14.7	–	4.9	–	1.6	–	Leu[95]	14.8	15.5	2.5	2.9	5.8	5.8
Val[43]	–	15.1	–	4.9	–	1.6	Lys[96]	14.4	15.2	2.9	2.4	6.0	7.6
His[44]	14.6	15.3	3.5	3.9	7.2	7.6	His[97]	14.2	–	4.4	4.4	3.8	4.6
Asp[45]	–	16.4	–	2.9	–	1.6	Glu[98]	15.6	15.6	5.0	4.4	0.0	1.0
Cys[48]	–	14.8	–	2.4	–	4.8	Cys[101]	13.1	–	0.8	–	1.6	–
Asp[51]	–	16.2	–	4.4	–	8.8	Arg[102]	15.3	15.7	2.1	2.4	6.8	5.0
Glu[52]	–	15.0	–	2.9	–	6.0	Thr[103]	–	16.0	–	6.8	–	3.6
Glu[54]	–	14.2	–	2.9	–	6.0							

ducible within the given statistical error, corroborating the reliability of the method.

The coupling constants derived from this experiment do not suffer from differential relaxation (Harbison, 1993; Norwood, 1993a,b; Schmidt et al., 1994) that can occur with increasing molecular weight, since the T_1 times of the carbonyls are relatively long (~2 s) for medium-sized proteins (L.E. Kay (1994) personal communication). The long T_1 times result from the fact that neither heteronuclear dipolar nor CSA relaxation have a J(0) component (Abragam, 1961). ^{13}C-^{13}C dipolar interaction, which has a J(0) component, may falsify the extracted coupling constants only for molecules with correlation times greater than 100 ns.

Conclusions

In conclusion, the method we present here allows the measurement of the heteronuclear $^3J(H_i^N,C'_i)$, $^2J(H_i^N,C'_{i-1})$ and $^1J(N_i,C'_{i-1})$ couplings in a very sensitive, quick and reliable manner using two-dimensional experiments, provided the ^1H,^{15}N-HSQC experiment displays sufficient resolution. Introducing a third dimension helps to cope with overlap problems, without severely compromising the sensitivity of the experiments used for the coupling constant determination. A time-domain fitting procedure has been developed that allows an automated determination of the coupling constants. These coupling constants contain valuable structural and dynamical information

and will, together with the more commonly measured $^3J(H^N,H^\alpha)$ coupling constants, allow a more precise structure determination (Clore, 1994). In addition, the C'-FIDS-HSQC and -HNCO are considerably more sensitive than the Soft HNCA-COSY experiment (Seip et al., 1994; Weisemann et al., 1994; Löhr and Rüterjans, 1995) that yields the $^3J(H_i^N,C_i')$ coupling based on the E.COSY principle. Furthermore, the method proposed here can also be used for the measurement of other heteronuclear coupling constants, e.g. those related to the angles χ and ψ in proteins.

Acknowledgements

This work was supported by the DFG under Grant Gr 1211/2-3 and by the Fonds der Chemischen Industrie. A.R. acknowledges a grant from the Fonds der Chemischen Industrie and is a member of the DFG-Graduiertenkolleg Eg 52/3-3, Institut für Organische Chemie, Universität Frankfurt am Main, Germany. H.S. is supported by an EC fellowship ('Human Capital and Mobility'). We are grateful to Dr. U. Weydemann (Rhein Biotech, Düsseldorf, Germany) who prepared the sample of rhodniin and to M. Maurer and V. Bellinger for providing the assignment of chemical shifts of rhodniin.

References

Abragam, A. (1961) *Principles of Nuclear Magnetism*, Clarendon Press, Oxford.

Bax, A. and Ikura, M. (1991) *J. Biomol. NMR*, **1**, 99–104.

Bax, A., Max, D. and Zax, D. (1992) *J. Am. Chem. Soc.*, **114**, 6924–6925.

Blake, P.R., Summers, M.F., Adams, M.W.W., Park, J.-B. and Bax, A. (1992) *J. Biomol. NMR*, **2**, 527–533.

Clore, G.M. (1994) *J. Magn. Reson. Ser. B*, **104**, 99–103.

Delaglio, F., Torchia, D.A. and Bax, A. (1991) *J. Biomol. NMR*, **1**, 439–446.

Edison, A.S., Markley, J.L. and Weinhold, F. (1994a) *J. Biomol. NMR*, **4**, 519–542.

Edison, A.S., Weinhold, F., Westler, W.M. and Markley, J.L. (1994b) *J. Biomol. NMR*, **4**, 543–551.

Eggenberger, U., Schmidt, P., Sattler, M., Glaser, S.J. and Griesinger, C. (1992a) *J. Magn. Reson.*, **100**, 604–610.

Eggenberger, U., Karimi-Nejad, Y., Thüring, H., Rüterjans, H. and Griesinger, C. (1992b) *J. Biomol. NMR*, **2**, 583–590.

Emsley, L. and Bodenhausen, G. (1989) *J. Magn. Reson.*, **82**, 211–221.

Emsley, L. and Bodenhausen, G. (1990) *Chem. Phys. Lett.*, **165**, 469–476.

Garrett, D.S., Kuszewski, J., Hancock, T.J., Lodi, P.J., Vuister, G.W., Gronenborn, A.M. and Clore, G.M. (1994) *J. Magn. Reson. Ser. B*, **104**, 99–103.

Griesinger, C., Sørensen, O.W. and Ernst, R.R. (1985) *J. Am. Chem. Soc.*, **107**, 6394–6396.

Griesinger, C., Sørensen, O.W. and Ernst, R.R. (1986) *J. Chem. Phys.*, **85**, 6837–6852.

Griesinger, C., Sørensen, O.W. and Ernst, R.R. (1987) *J. Magn. Reson.*, **75**, 474–492.

Grzesiek, S. and Bax, A. (1993) *J. Biomol. NMR*, **3**, 185–204.

Grzesiek, S., Vuister, G.W. and Bax, A. (1993) *J. Biomol. NMR*, **3**, 487–493.

Harbison, G.S. (1993) *J. Am. Chem. Soc.*, **115**, 3026–3027.

Juranic, N., Ilich, P.K. and Macura, S. (1995) *J. Am. Chem. Soc.*, **117**, 405–409.

Karimi-Nejad, Y., Schmidt, J.M., Rüterjans, H., Schwalbe, H. and Griesinger, C. (1994) *Biochemistry*, **33**, 5481–5492.

Kay, L.E., Ikura, M., Tschudin, R. and Bax, A. (1990) *J. Magn. Reson.*, **89**, 496–514.

Keeler, J., Neuhaus, D. and Titman, J.J. (1988) *Chem. Phys. Lett.*, **146**, 545–548.

Keeler, J., Neuhaus, D. and Titman, J.J. (1989) *J. Magn. Reson.*, **85**, 111–131.

Keeler, J. and Titman, J.J. (1990) *J. Magn. Reson.*, **89**, 640–646.

Löhr, F. and Rüterjans, H. (1995) *J. Biomol. NMR*, **5**, 25–36.

Madsen, J.C., Sørensen, O.W., Sørensen, P. and Poulsen, F.M. (1993) *J. Biomol. NMR*, **3**, 239–244.

Muhandiram, D.R., Xu, G.Y. and Kay, L.E. (1993) *J. Biomol. NMR*, **3**, 463–470.

Muhandiram, D.R. and Kay, L.E. (1994) *J. Magn. Reson. Ser. B*, **103**, 203–216.

Neri, D., Szyperski, T., Otting, G., Senn, H. and Wüthrich, K. (1989) *Biochemistry*, **28**, 7511–7516.

Norwood, T.J. (1993a) *J. Magn. Reson. Ser. A*, **101**, 109–112.

Norwood, T.J. (1993b) *J. Magn. Reson. Ser. A*, **104**, 106–110.

Palmer III, A., Cavanagh, J., Wright, P.E. and Rance, M. (1991) *J. Magn. Reson.*, **93**, 151–170.

Schleucher, J., Sattler, M. and Griesinger, C. (1993) *Angew. Chem.*, **105**, 1518–1521.

Schmidt, P., Schwalbe, H. and Griesinger, C. (1994) Poster WP 114, 35th ENC, April 10–15, 1994, Asilomar, CA.

Schwalbe, H., Samstag, W., Engels, J.W., Bermel, W. and Griesinger, C. (1993) *J. Biomol. NMR*, **3**, 479–486.

Schwalbe, H., Marino, J.P., King, G.C., Wechselberger, R., Bermel, W. and Griesinger, C. (1994) *J. Biomol. NMR*, **4**, 631–644.

Seip, S., Balbach, J. and Kessler, H. (1994) *J. Magn. Reson. Ser. B*, **104**, 172–179.

Shaka, A.J., Barker, P.B. and Freeman, R. (1985) *J. Magn. Reson.*, **64**, 547–552.

Vuister, G.W. and Bax, A. (1993a) *J. Am. Chem. Soc.*, **115**, 7772–7777.

Vuister, G.W. and Bax, A. (1993b) *J. Magn. Reson. Ser. B*, **102**, 228–231.

Vuister, G.W., Wang, A.C. and Bax, A. (1993a) *J. Am. Chem. Soc.*, **115**, 5334–5335.

Vuister, G.W., Yamazaki, T., Torchia, D.A. and Bax, A. (1993b) *J. Biomol. NMR*, **3**, 297–306.

Weisemann, R., Rüterjans, H., Schwalbe, H., Schleucher, J., Bermel, W. and Griesinger, C. (1994) *J. Biomol. NMR*, **4**, 231–240.

Zhu, G. and Bax, A. (1993) *J. Magn. Reson. Ser. A*, **104**, 353–360.